REFERENCES

1. Pagano, N. J. and H. T. Hahn. 1977. "Evaluation of Composite Curing Stresses," *Composite Materials: Testing and Design, 4th Conference*, ASTM STP 617:317–329.
2. Jones, R. M. 1975. *Mechanics of Composite Materials*, McGraw-Hill Co.
3. Tsai, S. W. and H. T. Hahn. 1980. *Introduction to Composite Materials*, Technomic Publishing Co., Inc., pp. 342–357.
4. Hyer, M. W. 1981. "Calculations of the Room Temperature Shapes of Unsymmetric Laminates," *J. Composite Materials*, 44:296–310.
5. Jun, W. J. and C. S. Hong. 1990. "Effect of Residual Shear Strain on the Cured Shape of Unsymmetric Cross-Ply Thin Laminates," *Comp. Science and Technology*, 38:55–67.
6. Peeters, L. J. B., P. C. Powell and L. Warnet. 1996. "Thermally-Induced Shapes of Unsymmetric Laminates," *J. Composite Materials*, 30:603–626.
7. White, S. R. and H. T. Hahn. 1993. "Cure Cycle Optimization for the Reduction of Processing Induced Residual Stresses in Composite Materials," *J. Composite Materials*, 27:1352–1376.
8. Unger, W. J. and J. S. Hansen. 1993. "The Effect of Cooling and Annealing on Residual Stress Development in Graphite Fiber Reinforced PEEK Laminates," *J. Composite Materials*, 27:108–137.
9. Reddy, J. N. 1984. "A Simple Higher-Order Theory for Laminated Composite Plates," *J. Appl. Mech.*, 51:745–752.
10. Hyer, M. W. 1981. "Some Observations on the Cured Shape of Thin Unsymmetric Laminates," *J. Composite Materials*, 15:175–194.
11. Strang, G. 1980. *Linear Algebra and Its Application*, Harcourt Brace Jovanovich, Inc.
12. Kim, M. H. 1996. "A Study on the Room-Temperature Curvature Shapes of Unsymmetric Laminates Including Slippage Effects," *M.S. Thesis*, Dept. of Aerospace Eng., Inha University, Korea.
13. Hyer, M. W. 1982. "The Room-Temperature Shapes of Four-Layer Unsymmetric Cross-Ply Laminates," *J. Composite Materials*, 16:318–340.

Prediction of Compression Strength of Unidirectional Polymer Matrix Composites

EVER J. BARBERO

Mechanical and Aerospace Engineering
West Virginia University
Morgantown, WV 26506-6106

(Received January 2, 1997)
(Revised July 29, 1997)

ABSTRACT: An analytical formulation is developed for the prediction of compression strength of unidirectional polymer matrix composites. The exact solution of the problem is simplified into an explicit equation for compression strength. Then, a nondimensional group is identified and used to propose a simple formula for the prediction of compression strength. The final formula can be used in design or to estimate the compression strength of production parts without performing compression testing. No empirical or semi-empirical parameters are used. The formula is validated for a broad class of materials including a variety of polymer matrices reinforced with carbon and glass fibers. Three parameters are required: the shear stiffness and strength of the composite and the standard deviation of fiber misalignment in the composite. All three parameters can be measured by well-established techniques. Data from the literature is used to validate the formula.

KEY WORDS: compression strength, unidirectional composite, polymer matrix composite, design equation.

1. INTRODUCTION

MANY MODELS HAVE been proposed trying to improve the prediction of compression strength of composites first introduced by Rosen [1]. The literature encompasses fiber buckling modes [2], kink-band models [3], and kink-bands induced by microbuckling [4]. In fiber buckling models, it is assumed that buckling of the fibers initiates a process that leads to the collapse of the material [1]. Rosen's model has been refined with the addition of initial fiber misalignment and non-linear shear stiffness [2]. The detrimental influence of fiber misalignment has been experimentally dem-

0021-9983/98/05 0483–20 $10.00/0

onstrated [5,6]. The experimental evidence suggests that fiber buckling of perfectly aligned fibers (Rosen's model) is an imperfection sensitive problem. Therefore, small amounts of imperfection (misalignment) could cause large reductions in the buckling load, thus the reduction of the compression strength with respect to Rosen's prediction. Fiber buckling can be shown to be insensitive to imperfections if a linear shear stress-strain law is used for the composite [7]. However, it has been shown [8] that imperfection sensitivity does occur for composites with non-linear shear response. The effect of initial shear stiffness on the compression strength has been studied experimentally [6,9], concluding that higher initial shear stiffness correlates with higher compression strength.

It has been shown [10–12] that the spacial distribution of fiber imperfections may affect significantly the compression strength of the composite. However, most fiber buckling models are deterministic with respect to fiber misalignment, in the sense that all the fibers are assumed to have a single value of fiber misalignment. Then, fiber misalignment is taken as an empirical parameter and it is set to a reasonable value so that the model predictions match the experimental data. By performing tests at different temperatures, effectively changing the shear response, Wang [2] shows that after the fiber misalignment is found empirically (by fitting measured strength data), it can be considered constant for a material. However, it is well known that there is not a unique value for fiber misalignment for all the fibers [13] but a Gaussian distribution of misalignment [14].

The standard deviation is a measure of the dispersion, not of the expected value of a distribution. However, it has been used [15], as a single misalignment value in the theoretical models. From a purely statistical point of view, the expected value (mean) of a distribution is a representative measure of the population. However, the expected value of the fiber misalignment distribution is zero [13]. The expected value of the half-normal distribution has also been used [15], but the predicted values compare reasonably well with experimental data only for a few materials. Continuous damage mechanics (CDM) was used [14] to combine the Gaussian distribution of misalignment with a deterministic model for compression strength. CDM predictions compare well with compression strength data for a broad class of materials.

The objective of this work is to develop an explicit equation to predict compression strength of Polymer Matrix Composites as a function of measurable parameters. The formula should not contain empirically adjustable factors and be simple enough to be used in practice.

2. COMPOSITE SHEAR RESPONSE

The shear stress-strain response of polymer-matrix composites can be represented [14,16] by

$$\tau = \tau_u \tanh\left(\frac{G_{LT}}{\tau_u}\gamma\right) \tag{1}$$

where G_{LT} is the initial shear stiffness and τ_u is the shear strength. The coefficients G_{LT} and τ_u are obtained by fitting the stress-strain experimental data. Complete polynomial expansions [17] fit the experimental data well but they are not anti-symmetric with respect to the origin. This introduces an artificial asymmetrical bifurcation during the stability analysis [8]. Asymmetrical bifurcation means that, because of the shear equation used, a straight fiber would have a preference for buckling with lateral deflections to one side and not to the other, which is physically unrealistic. Truncated polynomial expansions of the hyperbolic tangent preserve the anti-symmetry but they do not fit the data correctly for large values of strain.

For this paper, experimental values of G_{LT} and τ_u were taken from the literature. Experimental data can be obtained by a variety of techniques including the ± 45 coupon, 10° off-axis, rail shear, Iosipescu, Arcan, and torsion tests [18,19]. When experimental compression data is compared with model results, the non-linear shear stress-strain curve should be measured for the actual composite being tested in compression. We purposefully avoided using micromechanical models based on linear elasticity because the material exhibited non-linear behavior and because the in-situ properties of the matrix are different from the properties of the bulk matrix.

3. FIBER MISALIGNMENT

An optical technique [13] can be used to measure the misalignment angle of each fiber in the cross section. The technique consists of cutting the composite at an angle and measuring the major axis of the ellipse formed by the intersection of a cylindrical fiber with the cutting plane. The misalignment angle is computed from the major axis length, the fiber diameter (which can be measured as the minor axis of the ellipse), and the angle of the cutting plane. In this way, a distribution of fiber misalignment is obtained. The distribution was shown to be Gaussian by using the Cumulative Distribution Function (CDF) plot and the probability plot [14]. Therefore, the probability density (Figure 1) is

$$f(\alpha) = \frac{1}{\Omega\sqrt{2\pi}} \exp\left(\frac{-\alpha^2}{2\Omega^2}\right), \quad -\infty < \alpha < \infty \tag{2}$$

where Ω is the standard deviation and α is the continuous random variable, in this case being equal to the misalignment angle. The Cumulative Distribution Func-

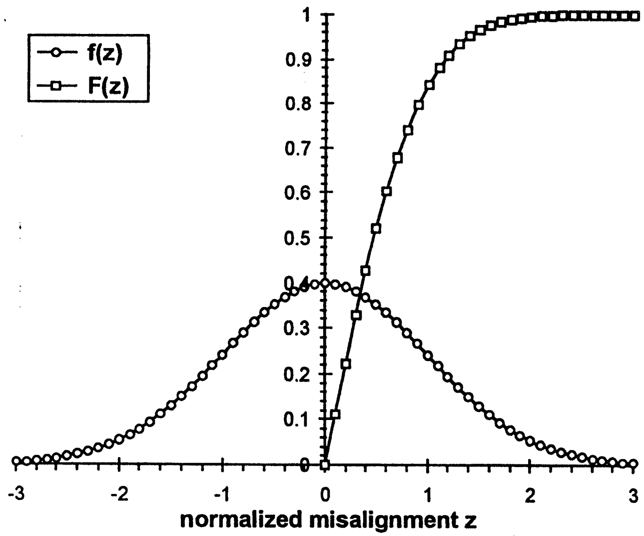

Figure 1. *Standard probability density function f(z), and F(z) vs. the normalized misalignment angle z.*

tion gives the probability of obtaining a value smaller than or equal to some value α. In terms of the normal distribution, the CDF is given by

$$\int_{-\infty}^{\alpha} f(\alpha')d\alpha' \tag{3}$$

where $f(\alpha')$ is the density of the normal distribution [Equation (2)]. Equation (2) represents the probability that a fiber picked at random in the cross section has a misalignment of value α. But more importantly, assuming that the number of fibers in the cross section is large [20,21], Equation (2) gives the ratio of the number of fibers that have a misalignment α over the total number of fibers. By having a large number of fibers in the cross section, there is certainty that a number of fibers with misalignment α will be found. From the statistical representation, it is not possible to say which fibers have that particular value of misalignment but it is possible to assert that a number of them, proportional to $f(\alpha)$, are present in the cross section.

For the computations, it is convenient to normalize the distribution in terms of a new variable z defined as

$$z = \frac{\alpha}{\Omega\sqrt{2}} \tag{4}$$

Then, the standard probability density function is

$$f(z) = \frac{\exp(-z^2)}{\Omega\sqrt{2\pi}} \tag{5}$$

The following integral, that is needed in the computations,

$$F(\alpha) = \int_{-\alpha}^{\alpha} f(\alpha')d\alpha'$$

can be readily expressed in terms of the normalized misalignment z as

$$F(z) = \text{erf }(z) = \frac{2}{\sqrt{\pi}}\int_0^z \exp(-z'^2)dz' \tag{6}$$

where erf (z) is the error function [22]. The functions $f(z)$ and $F(z)$ are plotted in Figure 1.

The standard deviation Ω of the normal distribution should not be used as a representative value of the population (fibers) because Ω represents a measure of the dispersion, not a representative value of the population. From a purely statistical point of view, a single value of misalignment that in the average represents the population is the expected value $E(\alpha)$ (or mean). However, the mean of the misalignment distribution is zero. To resolve this problem, it should be noted that fiber buckling occurs at the same load for positive or negative misalignment angle. Therefore, it may be useful to convert the symmetric normal distribution to a half normal. In the half normal distribution, the random variable is given as $x = abs(\alpha)$, where α is the random variable of the normal distribution. In other words, the half normal distribution represents the normal distribution without the algebraic sign (negative side gets folded onto the positive side). Using the new random variable x, the density of the half normal distribution is derived as

$$h(x) = \frac{1}{\Omega}\sqrt{\frac{2}{\pi}}\exp\left(\frac{-x^2}{2\Omega^2}\right); \quad x \geq 0 \tag{7}$$

The expected value of a half normal distribution is

$$E(x) = \int_{x=0}^{x=\infty} \frac{1}{\Omega}\sqrt{\frac{2}{\pi}}\exp\left(\frac{-x'^2}{2\Omega^2}\right)x'dx' = \sqrt{\frac{2}{\pi}}\,\Omega \tag{8}$$

However, using the expected value of the half-normal distribution did not lead to a good correlation with experimental data. This means that the process of compression failure cannot be modeled simply by averaging the misalignment distribution (see Appendix).

4. IMPERFECTION SENSITIVITY EQUATION

The relationship between the buckling stress and the imperfection (misalignment) is known in stability theory as the imperfection sensitivity curve. Several models from the literature can be used to develop this type of curve. A deterministic model, similar to the one presented by Wang [2] is developed here but using the representation of the shear response given by Equation (1). Unlike equilibrium-based models that compute the shear strain only at the inflection points of the fiber shape (Figure 2), the shear strain energy of the entire RVE is represented in the energy formulation used in this section. The assumption of same misalignment for all the fibers is implicitly accepted in all models existing in the literature that use a representation volume element (RVE).

The model presented in this section is based on the principal of total potential energy and, for simplicity, axial effects are assumed negligible. The potential energy of an elastic system is the sum of the elastic energy stored in the volume V plus the work done by the external forces over the surface S

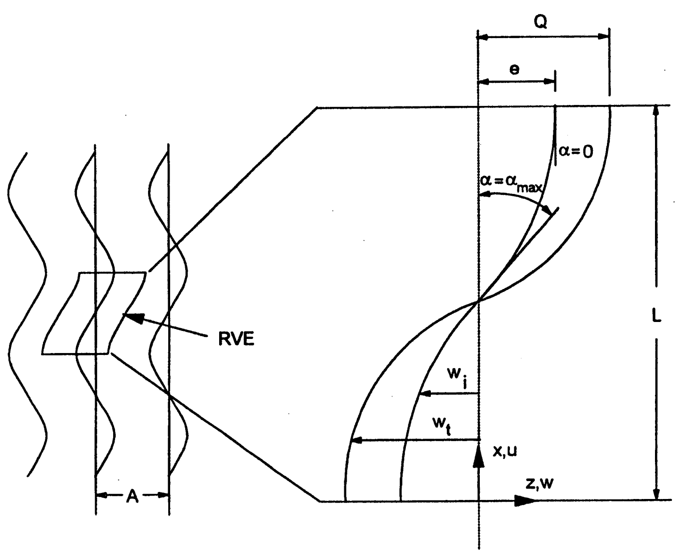

Figure 2. Representative Volume Element and variables used.

$$W = \int_V \int_0^{\varepsilon_{ij}} \sigma_{ij} d\varepsilon_{ij} dV - \int_S \hat{t}_i u_i dS$$

where σ_{ij} and ε_{ij} are the components of the stress and strain tensors, and u_i are the displacement components. For the one-dimensional system of Figure 2, where only the shear energy is considered the potential energy reduces to

$$W = \int_0^l \int_A \int_0^\gamma \tau d\gamma dA dx - P\Delta l$$

where P is the end load, Δl is the end shortening, τ and γ are the shear stress and strain, l and A are the length and area of the RVE. The end shortening can be computed as function of the total lateral deflection w_t (Figure 2) and the lateral deflection w_i caused by the imperfection (or waviness). Modeling the shear stress by Equation (1) we have

$$W = \int_0^l \int_A \int_0^\gamma \tau_u \tanh\left(\frac{\gamma G_{LT}}{\tau_u}\right) d\gamma dA dx - \frac{P}{2}\int_0^l \left(\left(\frac{dw_t}{dx}\right)^2 - \left(\frac{dw_i}{dx}\right)^2\right) dx$$

Next, we approximate the lateral deflections by

$$w_t = Q\cos\left(\frac{\pi x}{l}\right)$$

$$w_i = e\cos\left(\frac{\pi x}{l}\right)$$

where Q is the amplitude of the total lateral deflection of the fiber and e is the amplitude of the imperfection. The amplitude of the lateral deflections can be expressed in terms of the shear strain and the misalignment angle at the antinodes of the wavy shape of the buckled fiber (Figure 2) as

$$Q = \frac{\gamma l}{\pi} + e$$

$$e = \frac{\alpha l}{\pi}$$

Since the total potential energy has been discretized in terms of one degree of freedom Q, the equilibrium of the system is obtained by setting to zero the derivative of the load potential energy with respect to Q, and solving for the load P. Then, dividing by the area A, we obtain the equilibrium stress σ_{eq} as a function of the shear strain and the misalignment angle

$$\sigma_{eq}(\alpha,\gamma) = \frac{\tau_u}{2(\gamma+\alpha)} \cdot \frac{(\sqrt{2}-1)\left(e^{\sqrt{2}g} - e^{2g}\right) + (\sqrt{2}+1)\left(e^{(2+\sqrt{2})g} - 1\right)}{1 + e^{2g} - e^{\sqrt{2}g} + e^{(2+\sqrt{2})g}}$$

$$g = \gamma G_{LT}/\tau_u \tag{9}$$

with G_{LT} and τ_u as parameters. Typical results are shown in Figure 3 for Glass-Polyester with properties given in Table 1.

If the shear-strain plot is linear ($\tau = G_{LT}\gamma$) we obtain a stress-strain curve in compression described by

$$\sigma = \frac{G_{LT}\gamma}{\gamma + \alpha} \tag{10}$$

Note that if the shear behavior is assumed to be linear, Equation (10) predicts no critical value (maximum) of stress ($d\sigma/d\gamma \neq 0$ for $\gamma > 0$). On the contrary, by using

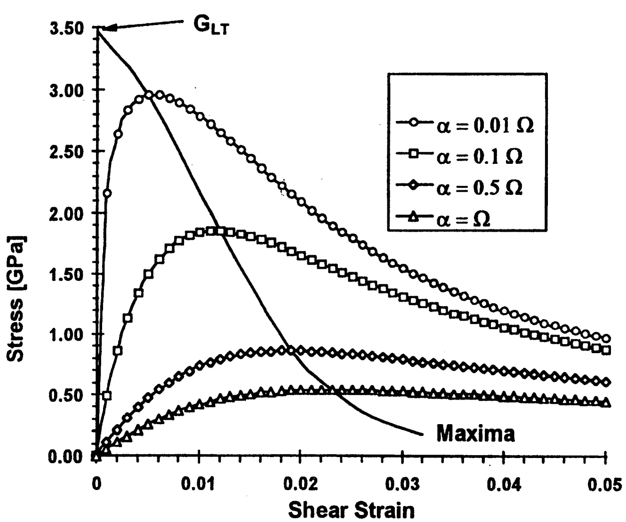

Figure 3. *Equilibrium states for various values of fiber misalignment.*

Table 1. ***Comparison of experimental data with predicted values.***

Material	V_f (%)	G_{LT} (MPa)	τ_u (MPa)	Ω (deg.)	χ	Experimental σ_c/G_{LT}	Approximate Formula σ_c/G_{LT}	Explicit Formula σ_c/G_{LT}	Numerical Solution σ_c/G_{LT}
XAS/914C	60*	5133	125	1.01	0.724	0.352	0.357	0.338	0.343
AS4/PEEK	61	5354	157.5	1.53	0.908	0.310	0.315	0.305	0.308
AS4/E7K8	60	7923.5	90.948	1.179	1.793	0.213	0.211	0.213	0.213
Glass-Vinyl Ester	43	4223	54.77	3.3	4.441	0.124	0.118	0.120	0.118
Glass-Polyester	40.2	3462	40.57	3.4567	5.148	0.138	0.107	0.108	0.104

*Estimated.

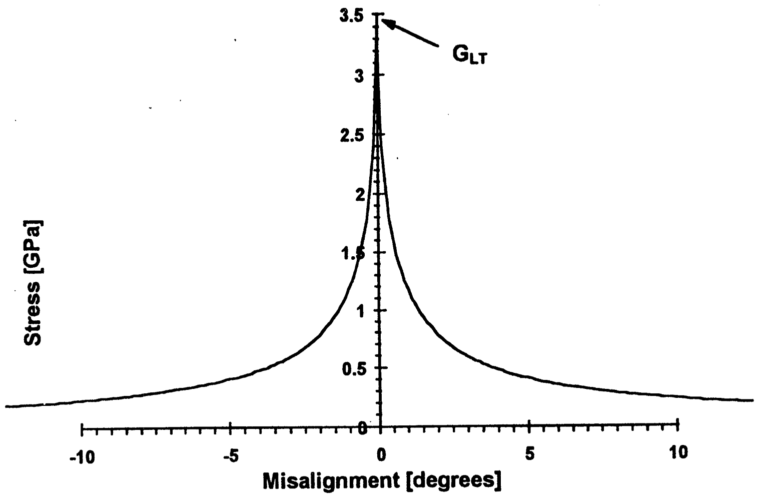

Figure 4. Imperfection sensitivity plot.

the hyperbolic tangent representation of shear [Equation (1)], a maximum is shown in Equation (9) and Figure 3 that corresponds to the compression strength for a particular angle of misalignment.

The maxima of the curves for all misalignment angles (shown in Figure 3) represents the imperfection sensitivity curve, as shown in Figure 4 for Glass-Polyester (Table 1). This curve represents the compression strength $\sigma(\alpha)$ of a fiber (and surrounding matrix) as function of its misalignment. For negative values of misalignment, it suffices to assume that the function is symmetric $(\sigma(-\alpha) = (\sigma(\alpha))$.

5. CONTINUUM DAMAGE MODEL

The stress carried by a fiber reduces rapidly after reaching its maximum, as illustrated in Figure 3, showing that the load carrying capacity of a buckled fiber is much lower than the applied load. Several models can be constructed depending of the assumed load that a fiber carries after buckling. A lower bound can be found assuming that buckled fibers carries no more load because they have no post-buckling strength.

According to the imperfection sensitivity curve in Figure 4, fibers with large misalignment buckle under low applied stress. If the post-buckling strength is assumed to be zero, the applied stress is redistributed onto the remaining, unbuckled fibers, which then carry a higher effective stress $\sigma(\alpha)$. At any time during loading of the specimen, the applied load $\bar{\sigma}$ (applied stress times initial fiber area) is equal to the effective stress times the area of fibers that remain unbuckled

$$\bar{\sigma} = \sigma(\alpha)[1 - \omega(\alpha)] \tag{11}$$

where $0 \leq \omega(\alpha) \leq 1$ is the area of the buckled fibers per unit of initial fiber area. For any value of effective stress, all fibers having more than the corresponding value of misalignment given in Figure 4 have buckled. The area of buckled fibers $\omega(\alpha)$ is proportional to the area under the normal distribution located beyond the misalignment angle $\pm\alpha$ (Figure 1). Therefore, $\omega(\alpha)$ is given by

$$\omega(\alpha) = 1 - \int_{-\alpha}^{\alpha} f(\alpha')d\alpha' = 2\int_{\alpha}^{\infty} f(\alpha')d\alpha' \tag{12}$$

taking into account that

$$\int_{-\infty}^{\infty} f(\alpha')d\alpha' = 1$$

Equation (11) has a maximum that corresponds to the maximum stress that can be applied to the composite, as shown in Figure 5. Therefore, the compression strength of the composite is found as

$$\sigma_c = \max\left[\sigma(\alpha)\int_{-\alpha}^{\alpha} f(\alpha')d\alpha'\right] \tag{13}$$

where $\sigma(\alpha)$ is given by Equation (9) and $f(\alpha')$ is given by Equation (2). The computations were carried out numerically and presented in Table 1 as σ_c/G_{LT} numerical. The maximum of Equation (11) given by Equation (13) is a unique value for the compression strength of the composite that incorporates both the imperfection sensitivity curve (Figure 4) and the distribution of fiber misalignment. Note that the standard deviation Ω is not arbitrarily chosen as a representative value of fiber misalignment for all the fibers but used just as a parameter to describe the actual distribution. Two alternative models are described in the Appendix.

6. EXPLICIT FORMULA

Since the distribution given in Equation (2) cannot be integrated in closed form [22], Equation (13) is evaluated numerically. However, it is advantageous to develop an explicit formula so that the compression strength can be easily predicted. The first step in the development of an explicit formula for compression strength is to simplify the shear stress-strain law [Equation (1)]. The hyperbolic tangent representation of the shear stress-strain data fits experimental data well [14,23]. Since

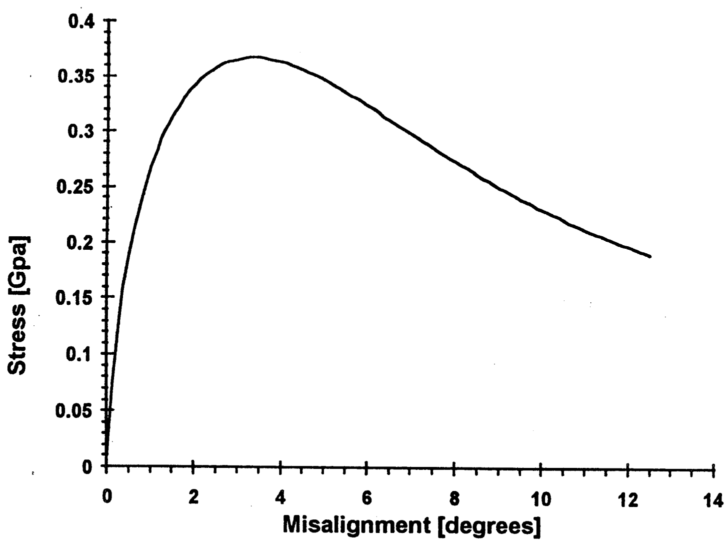

***Figure 5.** Applied stress $\bar{\sigma}$ as a function of misalignment. Loading of the sample proceeds from left to right, until compression failure at the apex of the plot.*

the use of the hyperbolic tangent leads to an involved equation for the equilibrium state [Equation (9)], the hyperbolic tangent is approximated with

$$\tau = G_{LT}\gamma + C_2\gamma^2 \tag{14}$$

The coefficient C_2 is found simply by matching one point on the curve as

$$C_2 = \frac{\tau_u}{\gamma_{\lim}^2}\tanh\left(\frac{G_{LT}}{\tau_u}\gamma_{\lim}\right) - \frac{G_{LT}}{\gamma_{\lim}} \tag{15}$$

where $\gamma_{\lim}$ is the value of shear strain, in the non-linear range, where the two curves are matched. Since a quadratic polynomial does not fit well a hyperbolic tangent for large values of shear strain, the fit must be done up to a value close to the shear strain in the composite when compression failure occurs [γ_{CR}, Equation (26)]. For most composite materials, including Carbon-Epoxy and Glass-Polyester, the fit should not extend beyond

$$\gamma_{\lim} = 2\frac{\tau_u}{G_{LT}} \tag{16}$$

This procedure provides an excellent approximation in the region of interest ($\gamma < \gamma_{CR} \leq \gamma_{\lim}$), as shown in Figure 6 for Glass-Polyester (Table 1).

Replacing Equation (16) into Equation (1) and taking into account that $\tanh(2) \approx 1$. We can write

$$C_2 = -\frac{G_{LT}^2}{4\tau_u} \tag{17}$$

Then, the shear stress-strain law [Equation (1) or Equation (14)] becomes

$$\tau = G_{LT}\gamma - \frac{G_{LT}^2}{4\tau_u}\gamma^2 \tag{18}$$

The equilibrium state for a given misalignment angle [Equation (9)] becomes

$$\sigma(\alpha,\gamma) = \frac{\gamma G_{LT}}{\gamma+\alpha} + \frac{8}{3}\frac{C_2\gamma^2}{(\gamma+\alpha)\pi} \tag{19}$$

Similarly, the imperfection sensitivity is

$$\sigma(\alpha) = \frac{4\sqrt{2}C_2\alpha\left(-8C_2\alpha + 3\pi G_{LT}\right)}{3\pi\sqrt{-C_2\alpha\left(-8C_2\alpha + 3\pi G_{LT}\right)}} - \frac{16C_2\alpha}{3\pi} + G_{LT}$$

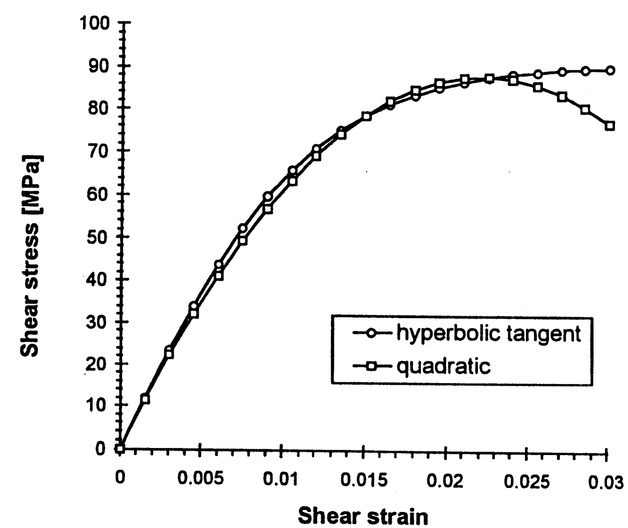

***Figure 6.** Fit of the hyperbolic tangent with a quadratic polynomial.*

or in terms of z

$$\sigma(z) = \frac{4\sqrt{2}C_2 z\sqrt{2}\Omega\left(-8C_2 z\sqrt{2}\Omega + 3\pi G_{LT}\right)}{3\pi\sqrt{-C_2 z\sqrt{2}\Omega\left(-8C_2 z\sqrt{2}\Omega + 3\pi G_{LT}\right)}} - \frac{16C_2 z\sqrt{2}\Omega}{3\pi} + G_{LT} \quad (20)$$

Since the integral of the normal probability function [Equation (6)] is a transcendental equation, it is approximated with a quadratic polynomial. An excellent fit is obtained using the interval $0 < \alpha < 3\Omega$. This interval is more than sufficient for the purpose at hand. Then, Equation (6) becomes

$$F(z) = 1.179643858\, z - 0.3455580967\, z^2 \quad (21)$$

The compression strength is found as the maximum of the applied stress

$$\overline{\sigma}(z) = \sigma(z)F(z) \quad (22)$$

To find the maximum explicitly, Equation (22) is expanded into a truncated polynomial. The best approximation, for a broad class of materials, is obtained expanding about $\alpha = \Omega\left(\text{or } z = 1/\sqrt{2}\right)$. The applied stress given by Equation (22) and the truncated polynomial expansion are shown in Figure 7 for AS4/E7K8 (Table 1). The root of the derivative of $\overline{\sigma}(z)$ with respect to z is found explicitly. In terms of misalignment, the root is the misalignment angle of the fibers that buckle just prior to compression failure. Its value is given by

$$\alpha_{CR} = \begin{bmatrix} 1019.011 G_{LT} C_2^2 \Omega^3 - 375.3162 C_2^3 \Omega^4 - 845.7457 G_{LT}^2 C_2 \Omega^2 \\ + g(282.1113 G_{LT} C_2 \Omega^2 - 148.1863 G_{LT}^2 \Omega - 132.6943 C_2^2 \Omega^3) \end{bmatrix}$$

$$\times \begin{bmatrix} 457.3229 C_2^3 \Omega^3 - 660.77 G_{LT} C_2^2 \Omega^2 - 22.43143 G_{LT}^2 C_2 \Omega \\ + g(161.6881 C_2^2 \Omega^2 - 138.3753 G_{LT} C_2 \Omega - 61.38939\, G_{LT}^2) \end{bmatrix}^{-1} \quad (23)$$

$$g = \sqrt{C_2\Omega(8.0 C_2\Omega - 9.424778 G_{LT})}$$

with C_2 given by Equation (17). Finally, using Equation (17) and replacing $z_{CR} = \alpha_{CR}/\sqrt{2\Omega^2}$ [Equation (4)] into Equation (22), we obtain the compression strength of the unidirectional composite, explicitly in terms of the standard deviation Ω of the fi-

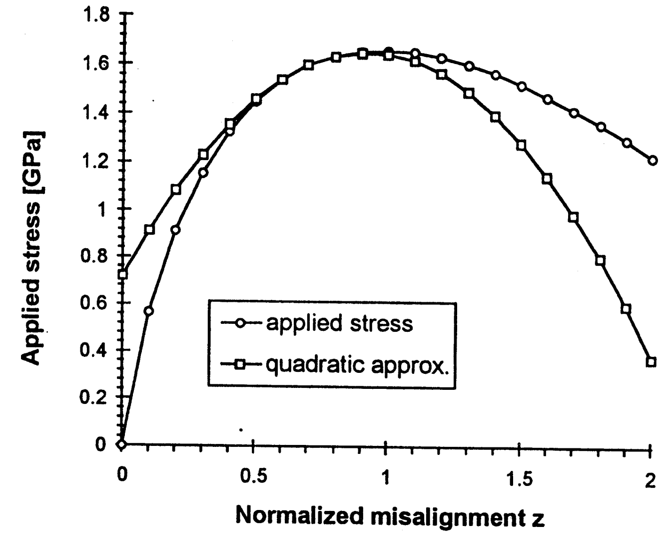

Figure 7. *Comparison of the applied stress $\overline{\sigma}$ [Equation (22)] and a truncated polynomial expansion, for AS4/E7K8.*

ber misalignment distribution, the in-plane shear stiffness G_{LT}, and the shear strength τ_u, as

$$\frac{\sigma_c}{G_{LT}} = \frac{\chi}{24\pi}\frac{a}{b}$$

$$a = -10979.6 - 8432.03\chi^2 - 19037.205\chi - 124.653\chi^4 - \frac{103961}{64}\chi^3$$

$$+ (12191.07 + 1881.87\chi^2 + 176.286\chi^3 + 7979.978\chi)\sqrt{\frac{\chi^2}{2} + 2.356\chi} \quad (24)$$

$$b = \left(-7.146\chi^3 - 41.298\chi^2 + 5.608\chi\right)\sqrt{\frac{\chi^2}{2} + 2.356\chi}$$

$$+ \left(10.106\chi^2 + 34.594\chi - 61.389\right)\left(\frac{\chi^2}{2} + 2.356\chi\right)$$

with the dimensionless group χ given by

$$\chi = \frac{G_{LT}\Omega}{\tau_u} \tag{25}$$

Additionally, the shear strain at failure is

$$\gamma_{CR} = -\alpha_{CR} + \sqrt{\alpha_{CR^2} + \frac{3}{2}\frac{\pi\tau_u\alpha_{CR}}{G_{LT}}} \tag{26}$$

Equation (24) approximates very well the numerical solution of the exact problem [Equation (13)]. Furthermore, Equation (24) allows us to identify the dimensionless number $\chi = G_{LT}\Omega/\tau_u$ which indicates that the dimensionless compression strength σ_c/G_{LT} can be modeled in terms of only one dimensionless number (i.e., χ) instead of three variables (i.e., G_{LT}, τ_u, and Ω). This observation has significant implications for the experimental characterization of compression strength of composite materials. In fact, experimentation can be carried out for various values of the dimensionless number χ, with the results being relevant for any combination of the variables that enter in the dimensionless number, regardless of the specific values of G_{LT}, τ_u, and Ω used in the experiment [24]. For example, a full factorial experimental design [25] with three variables (i.e., G_{LT}, τ_u, and Ω), $m = 3$ levels of each variable, and $n = 4$ replicates requires $m^3n = 108$ experiments. Using the dimensionless number χ, with the same number of levels and replicates, only twelve experiments are required.

Taking into account that the dimensionless compression strength can be modeled in terms of the dimensionless number χ, the following simple equation is proposed

$$\frac{\sigma_c}{G_{LT}} = \left(\frac{\chi}{a} + 1\right)^b \tag{27}$$

where $a = 0.21$ and $b = -0.69$ are two constants chosen to fit either the numerical solution to the exact problem [Equation (13)] or the explicit equation [Equation (24)]. Note that Equation (27) is not an empirical equation, since no experimental data of compression strength has been used in its derivation. Equation (27) fits well the values predicted with explicit formula, as well as experimental data, as it can be observed in Figure 8.

To find the constants a and b, we constructed a full factorial design with three levels on the three original variables G_{LT}, τ_u, and Ω. This gives $n = 3^3 = 27$ points for which the dimensionless compression strength was computed using both Equation (24) and the numerical solution of Equation (13). Since both proce-

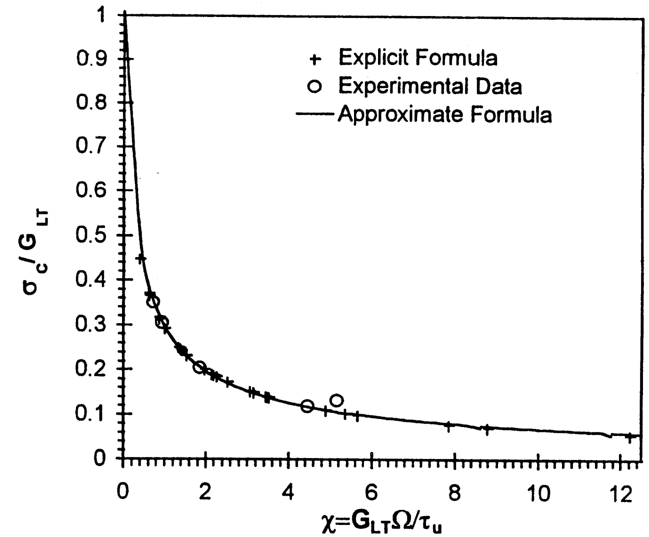

Figure 8. *Nondimensional compression strength as a function of the nondimensional number.*

dures give almost identical results, either one can be used to find a and b. The full factorial design was performed in the following interval of the variables

$$3500 < G_{LT} < 8000 \text{ MPa}$$

$$40 < \tau_u < 160 \text{ MPa}$$

$$\frac{\pi}{180} < \Omega < 3.5\frac{\pi}{180}$$

with Ω in radians. The interval chosen spans measured properties on a variety of composites: from fiberglass reinforced polyester to carbon reinforced PEEK. Then, Equation (27) was fitted to the data by minimizing the normalized error

$$\min\left(\sum_{i=1}^{n}\frac{(e_i - o_i)^2}{e_i}\right)$$

where e_i and o_i are the expected [Equation (27)] and observed [Equation (24) or Equation (13)] values respectively.

A comparison of predicted compression strength with experimental data is presented in Table 1. Predicted values are very close to the experimental data. Two carbon-Epoxy systems are included. Compression strength (from MIL17 [26]), shear properties and misalignment measurements for AS4/E7K8 are listed in [23]. Data for XAS/914C (a prepreg system from Ciba Geigy using AS4 fibers) and AS4/PEEK is listed in References [15] and [27]. Data for Glass-Polyester and Glass-Vinyl Ester is from Reference [14].

7. CONCLUSIONS

A dimensionless number $\chi = G_{LT}\Omega/\tau_u$ was proposed and shown to control the description of the compression strength behavior. In terms of this number, a simple formula was proposed to predict the compression strength of polymer matrix composites. The dimensionless number and the formula use only three material parameters that can be measured by well established methodologies: the shear stiffness and strength of the composite, and the standard deviation of fiber misalignment. Predicted values agree closely with experimental compression data from the literature for a broad class of materials. These include carbon and glass fibers, two Epoxies, a thermoplastic (PEEK), a Vinyl Ester, and a low cost Polyester. The formula is useful for design and to estimate the compression strength of composite structures without performing compression tests. Misalignment distribution of a production part can be significantly different from that of laboratory coupon samples commonly used to establish compression strength values. Furthermore, it is very difficult to test compression strength of samples from production parts. This is because of the inherent difficulties of compression testing that make the results dependent of the fixture used, the method of sample preparation, and the dimensions of the sample. On the other hand, shear stiffness and strength are readily available for most materials systems or they can be obtained using standard testing methods. The misalignment distribution, that is influenced by the quality of fabrication, can be measured from sectioned samples from production parts, using a well established methodology. Finally, it is worth to emphasize that the formula proposed in this work is based on mechanics principles and it does not contain any empirical parameter.

ACKNOWLEDGEMENTS

My sincere appreciation to Julio Massa for his suggestions on statistical analysis, to Hani Salim for his help with dimensional analysis, and to J. G. Häberle and J. S. Tomblin for providing some of the experimental data.

APPENDIX

Two alternatives to the model presented in Section 5 are described next to pro-

vide bounds to the model presented in Section 5. First, from a purely statistical point of view, an approximation to the compression strength could be proposed assuming that the contribution to the compression strength of each fiber is given by $\sigma(\alpha)$ [Equation (9)]. Then, the compression strength can be found by adding the contribution of all the fibers having various misalignment angles, according to their probability $f(\alpha)$

$$\sigma_c = \int_{-\infty}^{\infty} \sigma(\alpha) f(\alpha) d\alpha \tag{28}$$

However, the weighted probability integral [Equation (28)] leads to unrealistically high values of strength. This is because the probability is higher for angles close to zero, and these correspond to very high values of strength (up to $\sigma_c = G_{LT}$). This indicates that in the process of compression failure, there is a catastrophic propagation of failure at a threshold load below that predicted by Equation (28). The threshold load is likely to be that given by Equation (13).

Second, an attempt was made to take into account the non-zero post-buckling load carried by the buckled fibers. As a first approximation, it was assumed that the post-buckling load would remain constant, and equal to the buckling load. With this assumption, the compression strength can be found by adding the contribution of the buckled fibers to Equation (11), and looking for the maximum

$$\sigma_c = \max\left[\sigma(\alpha)\int_{-\alpha}^{\alpha} f(\alpha')d\alpha' + 2\int_{\alpha}^{\infty} \sigma(\alpha')f(\alpha')d\alpha'\right] \tag{29}$$

However, assuming that the fibers retain their buckling strength eliminated the apex from the applied stress vs. angle plot, thus leading to unrealistic results. This confirms the fact that buckled fibers have negligible post-buckling strength (previously proved by stability theory [8]).

REFERENCES

1. Rosen, B. W. 1965. Chapter 3 in "Fiber Composite Materials," Metals Park, OH: American Society for Metals.
2. Wang, A. S. D. 1978. "A Non-linear Microbuckling Model Predicting the Compressive Strength of Unidirectional Composites," *ASME Winter Annual Meeting, ASME Paper 78-WA/Aero-1.*
3. Lagoudas, D. C. and A. M. Saleh. 1993. "Compressive Failure due to Kinking of Fibrous Composites," *Journal of Composite Materials,* 27:83–106.
4. Yin, W-L. 1992. *A New Theory of Kink Band Formation,* AIAA-92-2552-CP.
5. Mrse, A. and M. R. Piggott. 1990. "Relation Between Fibre Divagation and Compressive Properties of Fibre Composites," *35th International SAMPE Symposium,* April 2–5, pp. 2236–2244.
6. Yurgartis, S. W. and S. S. Sternstein. 1992. "Experiments to Reveal the Role of Matrix Properties

and Composite Microstructure in Longitudinal Compression Strength," *ASTM Symposium on Compression Response of Composite Structures*, November 16–17.

7. Maewal, A. 1981. "Post-buckling Behavior of a Periodically Laminated Medium in Compression," *International Journal of Solids and Structures*, 17:335–344.
8. Tomblin, J. S., L. A. Godoy and E. J. Barbero. 1997. "Imperfection Sensitivity of Fiber Micro-Buckling in Elastic-Nonlinear Polymer-Matrix Composites," *Int. J. Solid Struct.*, 34(13): 1667–1679.
9. Crasto, A. S. and R. Y. Kim. 1992. "The Effects of Constituent Properties on the Compression Strength of Advanced Composites," *ASTM Symposium on Compression Response of Composite Structures*, November 16–17.
10. Kyriakides, R., E. J. Arseculeratne, E. J. Perry and K. Liechti. 1995. "On the Compression Failure of Fiber Reinforced Composites," *I. J. Solid Structures*, 32(6/7):689–738.
11. Chung, I. and Y. Weitsman. 1994. "A Mechanics Model for the Compressive Response of Fiber Reinforced Composites," *Int. J. Solid Struct.*, 31(18):2519–2536.
12. Chung, I. and Y. Weitsman. 1995. "On the Buckling/Kinking Compressive Failure of Fibrous Composites," *J. Solid Structures, Int. J. Solid Struct.*, 32(16):2329–2344.
13. Yurgartis, S. W. 1987. "Measurement of Small Angle Fiber Misalignment in Continuous Fiber Composites," *Composites Science and Technology*, 30:279–293.
14. Barbero, E. J. and J. S. Tomblin. 1996. "A Damage Mechanics Model for Compression Strength of Composites," *Int. J. Solid Struct.*, 33(29):4379–4393.
15. Häberle, J. G. and F. L. Matthews. 1994. "A Micromechanics Model for Compressive Failure of Unidirectional Fibre-Reinforced Plastics," *Journal of Composite Materials*, 28(17):1618–1639.
16. Steif, P. S. 1990. "A Model for Kinking in Fiber Composites—Part I. Fiber Breakage Via Micro-Buckling," 26:549–561, and "II. Kink Band Formation," *Int. J. Solids Struct.*, 26:563–569.
17. Sun, C. T. and A. W. Jun. 1993. "Effect of Matrix Nonlinear Behavior on the Compressive Strength of Fiber Composites," *Mechanics of Thick Composites*, The 1st Joint meeting of the ASME—ASCE—SES: Meet'N'93. Charlottesville, VA. June 6–9, pp. 91–105.
18. Chaterjee, S., D. Adams and D. Oplinger. 1993. "Test Methods for Composites—A Status Report—Volume III: Shear Test Methods," *DOT/FAA/CT-93/17 Final Report.*
19. Adams, D. F. and E. Q. Lewis. 1994. "Current Status of Composite Material Shear Tests Methods," *SAMPE J.*, 31(6), Jan/Feb.
20. Barbero, E. J. and K. W. Kelly. 1993. "Predicting High Temperature Ultimate Strength of Continuous Fiber Metal Matrix Composites," *Journal of Composite Materials*, 27(12):1214–1235.
21. Kelly, K. and E. J. Barbero. 1993. "The Effects of Fiber Damage on the Longitudinal Creep of CFMMC," *Int. J. Solids Struct.*, 30(24):3417–3429.
22. Erdelyi, A. 1953. "Higher Transcendental Functions," Volume 2, McGraw-Hill, N.Y.
23. Tomblin, J. S. and E. J. Barbero. 1996. "A Damage Mechanics Model for Compressive Strength of Fiber Reinforced Composites," *ASTM Special Technical Publications STP 1242, ASTM 13th Symposium on Composite Materials: Testing and Design*, May 20–21, Orlando, FL.
24. Ipsen, D. C. 1960. "Units, Dimensions and Dimensionless Numbers," McGraw-Hill, N.Y.
25. Montgomery, D. C. 1991. "Design and Analysis of Experiments," Wiley, 3rd Ed.
26. MIL-HNDBK-17-2C. 1994. "Polymer Matrix Composites—Volume II," *Material Properties,"* Department of Defense, Washington, DC.
27. Häberle, J. G. 1991. "Strength and Failure Mechanisms of Unidirectional Carbon Fibre-Reinforced Plastics Under Axial Compression," Ph.D. thesis, Imperial College, London, UK.

EDITORIAL POLICY

"The primary purpose of the *Journal of Composite Materials* is to provide a permanent record of achievements in the science, technology, and economics of composite materials. Implicit in this objective is the recognition and appropriate publication of the accomplishments of all participating interests.

"Fulfillment of this purpose depends almost entirely upon the voluntary contribution of articulate, accurate, and authoritative manuscripts. In addition to the multiple reviewing of candidate manuscripts to assure high standards of technical veracity, editorial selectivity also involves consideration of the equitable coverage of the entire field.

"In further discharging its responsibilities, the journal endorses the content and programs of appropriate trade associations and professional societies, but asserts its independent role in both the recording and, if necessary, appraising of their activities."

INSTRUCTIONS FOR AUTHORS

Submitting Papers to the Journal:

1. Three copies should be submitted to Editor, H. Thomas Hahn, Journal of Composite Materials, Hughes Aircraft Co. Professor, University of California, Los Angeles, MANE Department, Eng. IV, Los Angeles, CA 90024-1597.
2. Title should be brief, followed by name, affiliation, address, country, and postal code (zip) of author(s). Indicate to whom correspondence and proofs should be sent, including a telephone number.
3. Include a 100-word abstract, key words, and author(s) biographies.
4. Submit three copies also of camera-ready drawings and glossy photographs. Drawings should be uniformly sized, if possible, planned for 50% reduction. Both line drawings and photographs must be called out in the text. Appropriate captions should all be typed on one sheet.
5. Journal and book references should be identified in the text by enclosing in brackets and should be numbered in order. Literature references should be listed at end of manuscript, using following style:

   Journal: Halpin, J. C. 1967. J. Cellular Plastics, 3:432-435.
   Book: Ouellette, R. P. and P. N. Cheremisinoff. 1985. Applications of Biotechnology. Lancaster, PA: Technomic Publishing Co., Inc.
6. Tables. Number consecutively and type on a numbered, separate page. Please use arabic numerals and supply a heading. Column headings should be explanatory and carry units (see example at right).
7. Units & Abbreviations. SI units should be used. English units or other equivalents should appear in parentheses if necessary.

Table 5. Comparison of state-of-the-art matrix resins with VPSP/BMI copolymers.

Resin System	Core Temp. (DSC peak), °C	T_E, °C	PDT(N_2) °C	Char Yield, %
Epoxy (MY720)	235	250	300	30
Bismaleimide (H795)	282	>400	400	48
VPSP/Bismaleimide copolymer				
C379: H795 = 1.9	245	>400	400	50
C379: H795 = 1.4	285	>400	400	53

8. Symbols. A list of symbols used and their meanings should be included if a large number of symbols appears in the text.
9. Proofreading and Reprints. Authors will receive galley or page proofs, which they should correct and return as soon as possible. Also submit key words of your contribution on separate sheet provided. This is important in helping us to construct the index. Authors will also receive a reprint order form.
10. Copyright Information. All journal articles are copyrighted in the name of the publisher, except in the event of prior copyright by an author.
11. Headings. Your article should be structured with headings. Normally two headings are used as follows:

    Main Subhead: DESIGN OF A MICROWAVE INSTALLATION
    Secondary Subhead: Principle of the Design Method

    If further subordination is required, please limit to no more than one, or two at the most.
12. Equations. Number equations with arabic numbers enclosed in parentheses at the right-hand margin. Type superscripts and subscripts clearly above or below the baseline, or mark them with a caret: T^{2} T_{a} T^{2}_{a}. Be sure that all symbols, letters, and numbers are distinguishable (e.g., "oh" or zero, one or lowercase "el," "vee" or Greek nu). Handwritten Greek letters should be identified by spelling them out in the margin.
13. Permissions. The author is responsible for obtaining releases from other publishers for Technomic Publishing Company, Inc. to publish material copyrighted by someone else.

GENERAL

The *Journal of Composite Materials* is not responsible for the views expressed by individual contributors in articles published in the Journal.